International Journal of Electronics Signals and Systems

Volume 3 | Issue 1 Article 10

July 2013

AN ADAPTIVE SAR IMAGE DESPECKLING ALGORITHM USING STATIONARY WAVELET TRANSFORM

AMLAN JYOTI DAS1
Dept. of Electronics & Communication Engineering, Gauhati University, Guwahati-14, Assam, amlandas78@gmail.com

ANJAN KUMAR TALUKDAR
Dept. of Electronics & Communication Engineering, Gauhati University, Guwahati-14, Assam, anjan.nov@gmail.com

Kandarpa Kumar Sarma
Department of Electronics and Communication Technology, Gauhati University, Guwahati, Assam-781014, kandarpaks@gmail.com

Recommended Citation

DAS1, AMLAN JYOTI; TALUKDAR, ANJAN KUMAR; and Sarma, Kandarpa Kumar (2013) "AN ADAPTIVE SAR IMAGE DESPECKLING ALGORITHM USING STATIONARY WAVELET TRANSFORM," *International Journal of Electronics Signals and Systems*: Vol. 3 : Iss. 1 , Article 10.
DOI: 10.47893/IJESS.2013.1136
Available at: https://www.interscience.in/ijess/vol3/iss1/10

AN ADAPTIVE SAR IMAGE DESPECKLING ALGORITHM USING STATIONARY WAVELET TRANSFORM

AMLAN JYOTI DAS[1], ANJAN KUMAR TALUKDAR[2] & KANDARPA KUMAR SARMA[3]

[1,2&3]Dept. of Electronics & Communication Engineering, Gauhati University, Guwahati-14, Assam
E-mail - amlandas78@gmail.com, anjan.nov@gmail.com, kandarpaks@gmail.com

Abstract- In this paper, we present a Stationary Wavelet Transform (SWT) based method for the purpose of despeckling the Synthetic Aperture radar (SAR) images by applying a maximum a posteriori probability (MAP) condition to estimate the noise free wavelet coefficients. The solution of the MAP estimator is based on the assumption that the wavelet coefficients have a known distribution. Rayleigh distribution is used for modeling the speckle noise and Laplacian distribution for modeling the statistics of the noise free wavelet coefficients for the purpose of designing the MAP estimator. Rayleigh distribution is used for modeling the speckle noise since speckle noise can be well described by it. The parameters required for MAP estimator is determined by the technique used for parameter estimation after SWT. The experimental results show that the proposed despeckling algorithm efficiently removes speckle noise from the SAR images.

Keywords*- Synnthetic aperture radar (SAR), despeckling, Stationary Wavelet Transform (SWT), Maximum a posteriori probability (MAP) Estimator.*

I. INTRODUCTION

Synthetic aperture radar (SAR) allows the acquisition of high resolution images of different places on the earth. It is a all-weather, day and night system. SAR images are corrupted by special kind of noise known as speckle noise, for which automatic interpretation of SAR data is very difficult. In a SAR image, speckle manifests itself similar to thermal noise, by a random pixel-to-pixel variation with statistical properties. Therefore, in many SAR image processing operations like segmentation, speckle filtering is a crucial preprocessing step [1]. Many denoising algorithms have been developed for despeckling SAR images by using the Lee filter [2], the Frost filter [3], LG-MAP filter [13], the Gamma MAP filter [4], and their variations [5], [6]. These filters usually exhibit well in despeckling the SAR images, but they fail to provide sharp edge features and details of the original SAR image [7].

Since SAR images are multiplicative in nature, so many wavelet-based despeckling algorithms apply the log-transform to SAR images to statistically convert the multiplicative noise to *additive* noise prior to applying further denoising technique [7], [8]. An exponential operation is applied to convert the log-transformed images back to the nonlogarithmic format after wavelet denoising [8].

Several solutions have been proposed in the recent years, based on maximum a posteriori probability (MAP) criteria and different distributions: the gamma distribution [9], the α-stable distribution [10], the Pearson system of distributions [11], and the generalized Gaussian (GG) [12], laplacian and gaussian distribution [13] etc. In [12], a MAP criterion is derived which is associated with the Generalized Gaussian distribution and is performed in the undecimated wavelet domain. In [13], a MAP criterion is derived by considering Gaussian distribution for modeling speckle noise and Laplacian distribution for modeling noise free wavelet coefficients. In [14], the noise-free image was approximated by a Gauss-Markov random field prior and the speckle noise was modeled using Gamma pdf.

Although Discrete Wavelet Transform (DWT) plays a major role in the area of image denoising and image compression, the downsampling operation involved in DWT results in a time-variant translation and has to face difficulties in restoring original image discontinuities in the wavelet domain. Therefore, to restore the translation invariance property, lost by classical DWT, Stationary Wavelet Transform (SWT) has been preferred in many techniques [11].

In this paper we propose an efficient SWT based despeckling method by using MAP estimation. We avoid the log-transform and applied the MAP estimation criteria used as in [13], based on Gaussian distribution for modeling the speckle noise and Laplacian distribution for modeling the noise free wavelet coefficients. The parameter estimation is done using the results of [11]. The despeckling algorithms were tested on Ku-Band SAR image of pipeline over the Rio Grande river near Albuquerque, New Mexico (1-m resolution) with dimensions of 256×256, and were compared, which gives a satisfactory result for the proposed algorithm.

This paper is organized as follows. In Section II, we describe statistical properties of SAR images, the two-dimensional (2-D) SWT algorithm, and signal modeling. In Section III, we have given a brief review of statistical characterization of wavelet coefficients and speckle noise. In Section IV we have shown the related work on MAP Estimator design. In Section V, the parameter estimation is described. Section VI provides a description of our algorithm and Section VII shows experimental results. Finally, a short conclusion is given.

II. STATISTICAL MODELS FOR SAR IMAGES

A. Statistical models for SAR images

Let G be the observed signal (intensity or amplitude), and F be the noise-free signal. Since speckle noise is multiplicative in nature, the observed signal can be expressed as where, F is the noise free image and U is the normalized fading speckle-noise random variable, following a Gamma distribution with unit mean and variance . Its pdf is given by

$$p(U) = \frac{L^L U^{L-1} e^{-LU}}{\Gamma(L)} \quad ,U \geq 0 \tag{1}$$

where denotes the gamma function.

The observed intensity *I* of an *L*-look image has the conditional pdf given by [5]

$$p_{(I|F)}\left(\frac{g}{f}\right) = \frac{1}{\Gamma(L)}\left(\frac{L}{f}\right)^L g^{L-1} e^{-Lg/f} \tag{2}$$

Where, represents an observed intensity value and is the corresponding actual intensity value. Amplitude which is the square root of intensity is distributed with the following pdf [5]:

$$p_{(A|F)}\left(\frac{g}{f}\right) = \frac{2}{\Gamma(L)}\left(\frac{L}{f}\right)^L g^{2L-1} e^{-Lg^2/f} \tag{3}$$

Note that, if in eqn. (2) and (3) gives the distribution of monolook intensity and amplitude, which are exponential and Rayleigh distributions, respectively.

B. Stationary Wavelet Transform

The SWT algorithm is simple and is close to DWT. Figure1 shows the 2-D SWT decomposition algorithm, where and are the highpass and lowpass filters at level , respectively. Also, it can be noted in the figure that the original image is and that the output of each decomposition level is applied to the input of the next level . As shown in Figure 1, the two filters and are upsampled by two from filters of the previous decomposition level and . It is a redundant transform as SWT does not include downsampling operations. More precisely, as DWT, for level 1, all the decimated DWT for a given signal can be derived by convolving the signal with the appropriate filters without downsampling it.

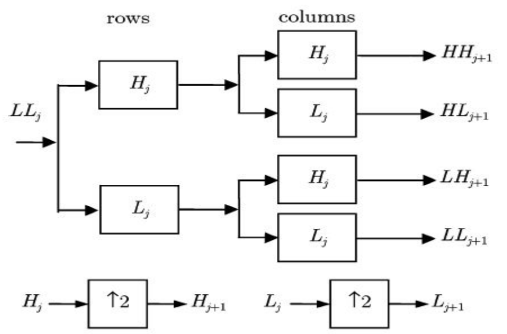

Figure 1: Block diagram of SWT Decomposition

C. Signal model

The observed signal is assumed to follow the following model:

$$g[n] = f[n].u[n] = f[n] + f[n].(u[n]-1) = f[n] + v[n] \tag{4}$$

where is the observed signal, is the speckle-free signal that we would like to estimate, is the speckle noise, and denotes the signal dependent speckle component in the equivalent additive model.

Let be the stationary wavelet operator applied to the signal *x*. It performs a multiresolution decomposition, where *j* is the decomposition level. We have,

$$W_g^{[j]}[n] = W_f^{[j]}[n] + W_v^{[j]}[n] \tag{5}$$

Despeckling an image in the multiresolution domain means estimation of the speckle noise free wavelet coefficients and applying the inverse stationary wavelet transform (ISWT) to obtain the noise free image.

III. STATISTICAL CHARACTERIZATION OF WAVELET COEFFICIENTS AND SPECKLE NOISE

The parametric MAP estimator presumes proper modeling of prior probability distribution of signal and speckle noise wavelet coefficients. In this paper, we model the signal component of the wavelet coefficients using the Laplacian distribution, and the Gaussian model is used for modeling the noise component.

D. Gaussian model for speckle component

The probability density function (pdf) for a Gaussian distributed random variable , is defined as [15]:

$$p_v(v) = \frac{1}{\sqrt{2\pi}\sigma_v} \exp\left(\frac{-(v-\mu_v)^2}{2{\sigma_v}^2}\right) \quad ,v \geq 0 \tag{6}$$

where, is the amplitude of the noise, is the standard deviation of noise and $\mu_v$is the mean of the noise

E. Laplacian model for Signal Component

The pdf of a Laplacian distributed random variable,f, defined as follows [13]

$$p_f(f) = \frac{1}{\sqrt{2}\sigma_f} e^{-\frac{\sqrt{2}|f-\mu_f|}{\sigma_f}} \quad (7)$$

where σ_f is the standard deviation of signal, f determines the spread of the density function and μ_f is the mean of the signal f.

IV. DESIGN OF THE PROPOSED MAP ESTIMATOR

The MAP estimator of the speckle-free wavelet coefficients is given by

$$\widehat{W}_f = \arg\max_{W_f} p(W_f|W_g) \quad (8)$$

After applying the Bayes rule and the log function, we have

$$\widehat{W}_f = \arg\max_{W_f}[\log p(W_f|W_g) + \log p(W_f) \quad (9)$$

The proposed method is based on (10) that, by using a simplified notation and the model in (5), can be rewritten as

$$\hat{\theta} = \arg\max_{W_f}[\log p_v(x-\theta) + \log p_\theta(\theta)] \quad (10)$$

where $\theta = W_f[n], x = W_g[n], and\ v = W_v[n]$

From eqn. (6) and (8), we have

$$p_v(x-\theta) = \frac{1}{\sqrt{2\pi}\sigma_v}\exp\left(\frac{-(x-\theta)^2}{2\sigma_v{}^2}\right) \quad (11)$$

And

$$p_\theta(\theta) = \frac{1}{\sqrt{2}\sigma_\theta} e^{-\frac{\sqrt{2}|\theta-\mu_\theta|}{\sigma_\theta}} \quad (12)$$

The MAP equation can be written as

$$\hat{\theta} = \arg\max_{W_f}\left[\log\frac{1}{\sqrt{2\pi}\sigma_v} e^{-\left(\frac{-(x-\theta)^2}{2\sigma_v{}^2}\right)} + \log\frac{1}{\sqrt{2}\sigma_\theta} e^{-\frac{\sqrt{2}|\theta-\mu_\theta|}{\sigma_\theta}}\right] \quad (13)$$

Taking $\frac{d\hat{\theta}}{d\theta}$ and equating it to zero, we have the solution

$$\hat{\theta} = x - \frac{\sqrt{2}\sigma_v{}^2}{\sigma_\theta} \quad (14)$$

The solution to this problem is given by:

$$\hat{\theta} = \begin{cases} x - \frac{\sqrt{2}\sigma_v{}^2}{\sigma_\theta} & , if\ x > \mu_\theta + \frac{\sqrt{2}\sigma_v{}^2}{\sigma_\theta} \\ x + \frac{\sqrt{2}\sigma_v{}^2}{\sigma_\theta} & , if\ x > \mu_\theta - \frac{\sqrt{2}\sigma_v{}^2}{\sigma_\theta} \\ \mu_\theta & , elsewhere \end{cases} \quad (15)$$

This solution is applied to the high frequency sub-bands (LH, HL, and HH) to estimate the noise free wavelet coefficients.

V. PARAMETER ESTIMATION FOR THE PROPOSED ESTIMATOR

In the solution of the MAP estimator there are three unknown parameters.

(i) μ_θ (Mean of the noise free wavelet coefficients):

$$\mu_\theta = E[\theta] = E[x] \quad (16)$$

(ii) σ_v^2: (noise variance): Based on the statistical properties of SWT transform and SAR images, Foucher *et al.* [8] estimate as

$$\sigma_v^2 = \psi_l \mu_x C_F(1 + C_\theta^2) \quad (17)$$

where, $\mu_x = E[x]\ and\ C_\theta^2$ is given by

$$C_\theta{}^2 = \frac{C_x{}^2 - \psi_l C_F{}^2}{\psi_l(1+C_F{}^2)} \quad (18)$$

where C_x is the normalized standard deviation of noisy wavelet coefficient and is given by

$$C_x = \frac{\sigma_x}{\mu_x} \quad (19)$$

Inserting (20) and (21) into (19), we obtain

$$\sigma_v{}^2 = \frac{C_F{}^2(\psi_l \quad \mu_x{}^2 + \sigma_x{}^2)}{1+C_F{}^2} \quad (20)$$

where C_F is the normalized standard deviation of noise and equals $\sqrt{1/L}$ for intensity images and $\sqrt{(4/\pi - 1)/L}$ for amplitude images $(L \geq 1)$, where L is the look of the SAR image, and parameter ψ_l is defined as

$$\psi_l = (\sum_k h_k{}^2)^2(\sum_k g_k{}^2)^{2(l-1)} \quad \text{(For diagonal subband)}$$
$$= (\sum_k h_k{}^2)^2(\sum_k g_k{}^2)^{2l-1} \quad \text{(For horizontal and vertical subband)} \quad (21)$$

where h and g are the highpass and lowpass filters at decomposition level l, respectively.

(iii) σ_θ^2 (Variance of the noise free wavelet coefficients): It can be calculated by using

$$\sigma_\theta{}^2 = \psi_l \mu_x{}^2 C_\theta{}^2 \qquad (22)$$

Using eqn. (16) - (22) the parameters are estimated for each high frequency subbands at each decomposition level.

VI. EXPERIMENTAL DETAILS

The block diagram of the proposed method is shown in Figure 2. The original noisy image is first transformed using SWT. From the SWT decomposed image the parameters mentioned in Section V are estimated using eqn. (16) - (22) for the high frequency subbands i.e. LH, HL, and HH subband at each decomposition level. These parameters are then used to calculate the solution of the MAP estimator using eqn. (15) for each high frequency subbands.

The solution of the MAP estimator is derived by using a prior knowledge for modeling the speckle noise and noise free wavelet coefficients. As described in Section III the speckle noise is modeled using Gaussian distribution and the signal component is modeled using Laplacian distribution. These conditions are then applied to each wavelet coefficients of LH, HL, and HH subband for the estimation of the noise free wavelet coefficients of the high frequency subbands using the conditions of the MAP estimator. These results the formation of high frequency subbands with the noise free estimated wavelet coefficients. Finally inverse SWT is taken for the low frequency subbands and the estimated high frequency subbands for each level. The results obtained by the proposed technique are shown in Figure 3. Some of the related works are reported in [17].

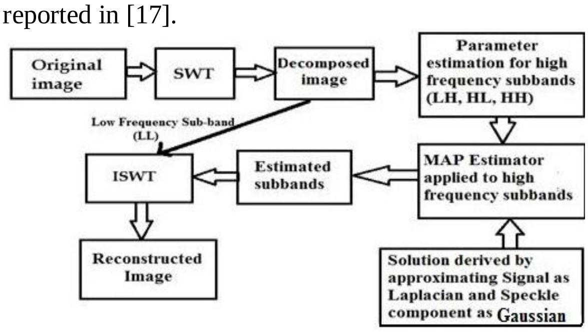

Figure 2: Block diagram of the proposed method.

VII. RESULTS AND DISCUSSION

For the purpose of comparison of the proposed technique we have considered the results that we have got by applying existing techniques like VisuShrink thresholding, BayesShrink thresholding, and Wiener filtering. Among the most popular thresholding methods include VisuShrink and BayesShrink. These thresholds take the advantage of asymptotic minimax optimalities over function spaces such as Besov spaces [16]. However, for image denoising, VisuShrink yield overly smoothed images. This is because its threshold choice, $\sigma\sqrt{2\log M}$ (called the *universal threshold* and is the noise variance), can be unwarrantedly large due to its dependence on the number of samples, which removes too many coefficients. VisuShrink provides a single value of threshold, which is globally applied to all the wavelet coefficients. The result of this method is shown in Figure 3(b) which shows that the quality of the image is worse than other methods like BayesShrink. The BayesShrink threshold is given by

$$T_{Bayes} = \sigma^2 / \sigma_B$$

where is the noise variance and is the standard deviation of noiseless coefficients in a subband. This threshold often provides a better denoising result than the SURE. The result is shown in Figure 3(c) which shows that, this method gives better result than VisuShrink but worse than other methods.

We have also made comparisons with the Wiener filter outputs, which was claimed to be the best linear filtering possible. The results are derived using the default settings (local window size), and the unknown noise power is estimated. The PSNR results are shown in Table I. They are considerably lower than the proposed method. The image quality (shown in Figure 3(d)) is also not as good as the techniques mentioned above.

The proposed method is compared with the existing methods like Bayes Shrink thresholding etc by comparing the corresponding PSNR values. The PSNR is defined as

$$PSNR = 10\log_{10}\frac{255^2(M.N)}{\sum_{i,j}(B(i,j)-A(i,j))^2}$$

where, □ is the denoised image, _ is the noise-free image and ( ) is the size of the denoised image. The comparison of the PSNR values is shown in Table I.

The PSNR is calculated for E-SAR images of Obepffafenhofen with different values of noise variance and applied to all the techniques which give a result as mentioned in Table I.

TABLE I. COMPARISION OF PSNR OF DIFFERENT DENOISING TECHNIQUE

INPUT PSNR	VISU SHRINK	BAYES SHRINK	WIENER FILTER	PROPOSED METHOD
27.6135	24.3189	24.4568	24.4756	28.3828
28.2838	24.1760	24.7860	24.8049	30.4351
29.7210	25.9526	26.3420	26.8564	30.9375
29.9965	26.0345	26.7834	26.9586	31.0219

It is seen that the proposed method has better PSNR for all the input images with different values of noise variance. Thus the proposed approach is suitable for SAR applications.

VIII. CONCLUSION

In this paper, an efficient technique for despeckling SAR images has been proposed. The speckle noise in the wavelet domain was modeled as an additive signal-dependent noise. We have tested the subband adaptive MAP processor, which relies on the Gaussian distribution of speckle noise and Laplacian prior for modeling the wavelet coefficients. Further, experimental results using the simulated speckled images show that, for five-level wavelet decompositions, the PSNR

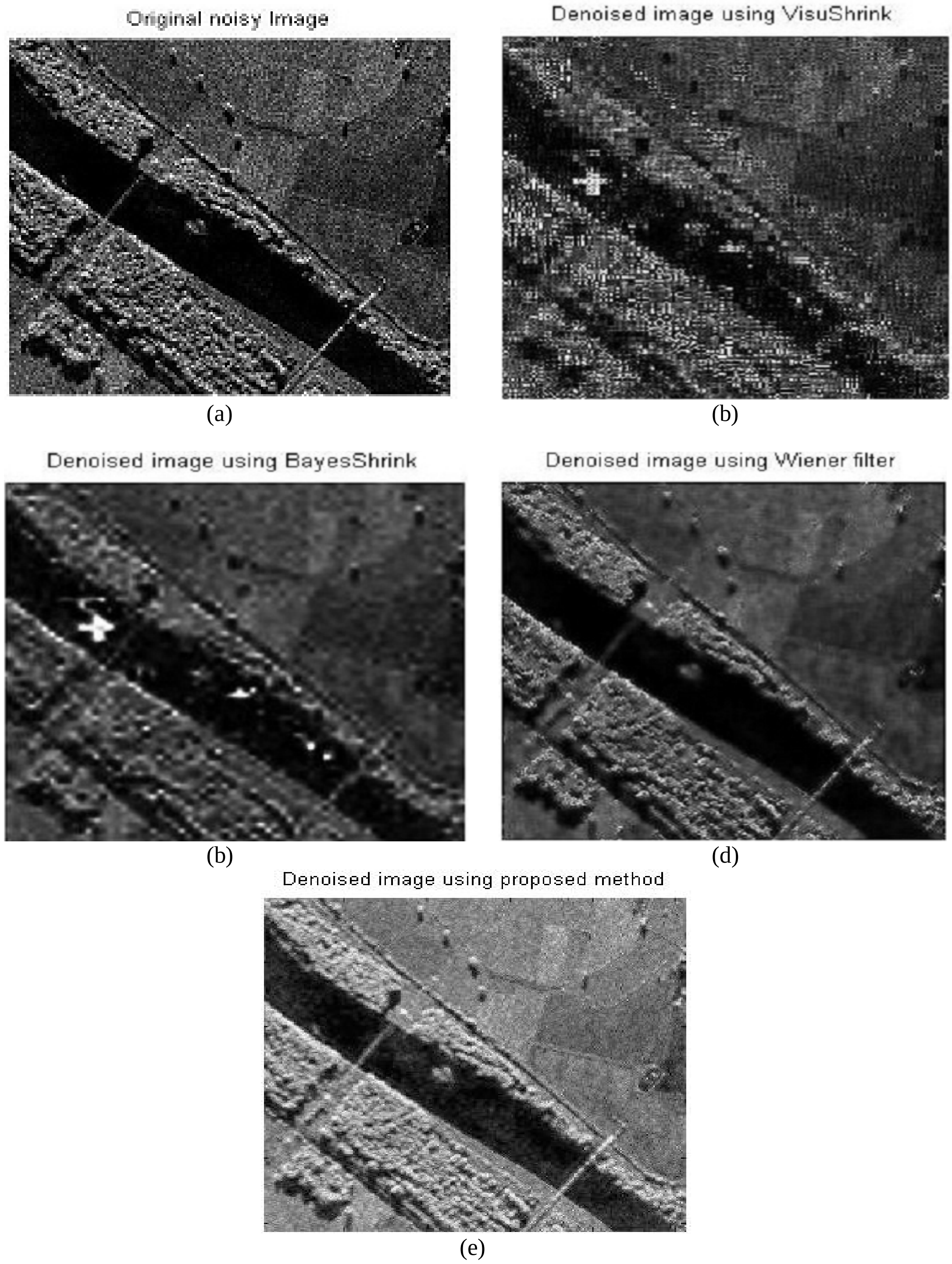

Figure 3: Original and denoised Ku-Band SAR image of pipeline over the Rio Grande river near Albuquerque, New Mexico: 1-m resolution. (a) Original noisy image (b) Denoised image using VisuShrink (c) Denoised image using BayesShrink (d) Denoised image using Wiener filter (e) Denoised

image using proposed method. values of the proposed technique are higher than those algorithms mentioned above at less computational complexity. Although the speckle noise is removed by a significant amount, the denoised SAR image is smoothed in each successive decomposition levels. The subsequent stage of the proposed method will be related to sharpening the edges so that more edge information can be restored, enhancing the resolution of the denoised image.

REFERENCES

[1] H. Xie, L. E. Pierce,and F. T. Ulaby "SAR speckle reduction using wavelet denoising," IEEE Transactions on Geoscience and Remote Sensing, Vol.40,No. 10, Oct. 2002.

[2] G. Lee, "Refined filtering of image noise using local statistics," *Comput.*

Graph. Image Process., vol. 15, no. 4, 1981.

[3] V. S. Frost, J. A. Stiles, K.S. Shanmugan, and J. C. Holtzman, "A model for radar images and its application to adaptive digital filtering of multiplicative noise," IEEE Trans. Pattern Anal. Machine Intell.,vol. PAMI-4, Mar. 1980.

[4] A. Lopes, E. Nezry, R. Touzi, and H. Laur, "Maximum a posteriori filtering and first order texture models in SAR images," in *Proc. IGARSS*, 1990.

[5] C. Oliver and S. Quegan, "Understanding synthetic aperture radar Images." Norwood, MA: Artech House, 1988.

[6] A. Lopes, R. Touzi, and E. Nezry, "Adaptive speckle filters and scene heterogeneity," IEEE Trans. Geosci. Remote Sensing, vol. 28, pp. 992-1000, Nov. 1990.

[7] L. Gagnon and A. Jouan, "Speckle filtering of SAR images- A comparative study between complex-wavelet-based and standard filters," Proc. SPIE, 1997.

[8] H. Guo, J. E. Odegard, M. Lang, R. A. Gopinath, I. W. Selesnick, and C. S. Burrus, "Wavelet based speckle reduction with application to SAR based ATD/R," in Proc. ICIP, 1994.

[9] S. Solbø and T. Eltoft, "Γ-WMAP: A statistical speckle filter operating in the wavelet domain." Int. J. Remote Sens., vol. 25, no. 5, pp. 1019-1036,Mar. 2004.

[10] A. Achim, P. Tsakalides, and A. Bezerianos, "SAR image denoising via Bayesian wavelet shrinkage based on heavy-tailed modeling," IEEE Trans. Geosci. Remote Sens., vol. 41 , no. 8, pp. 1773-1784, Aug. 2003.

[11] S. Foucher, G. B. Bénié, and J.-M. Boucher, "Multiscale MAP filtering of SAR images," IEEE Trans. Image Process., vol. 10, no. 1, pp. 49-60, Jan.2001.

[12] F. Argenti, T. Bianchi, and L. Alparone, "Multiresolution MAP despeckling of SAR images based on locally adaptive generalized Gaussian pdf modeling," IEEE Trans. Image Process., vol. 15, no. 11, pp.3385-3399.Nov.2006.

[13] F. Argenti, T. Bianchi, A. Lapini and L. Alparone, "Fast MAP despeckling based on Laplacian-Gaussian modelling of wavelet coefficients," IEEE Geoscience and Remote Sensing Letters, vol. 9, no. 1, Jan. 2012.

[14] M.Walessa and M. Datcu, "Model-based despeckling and information extraction from SAR images," IEEE Trans. Geosci. Remote Sens., vol. 38,no.5,pp.2258-2269,Sep.2000.

[15] Papoulis, A.: 'Probability random variables and stochastic processes' (MHL,NewYork,USA,1991).

[16] S. Grace Chang, Bin Yu, and Martin Vetterli, "Adaptive wavelet thresholding for image denoising and compression" IEEE Trans. On Image Processing, vol. 9, no. 9, Sept. 2000.

[17] A. J. Das, A. K. Talukdar, K. K. Sarma, "An adaptive stationary wavelet-based technique for despeckling SAR image", International Conference on Recent Developments in Computational Intelligence and Engineering Applications (RDCIEA), pp- 38-43, Guwahati, India, Dec, 2012.

[18] A. J. Das, A. K. Talukdar, K. K. Sarma, "A novel adaptive stationary wavelet based technique for SAR image despeckling", 1st International Conference on Mobile and Embedded Technology (MECON 2013), Noida, India, Jan, 2013.